

Identification of the Mechanical and Piezoelectric Parameters of a Massively Piezoelectric Structure

P. De Boe, R. Pascual, J.C. Golinval

Université de Liege, LTAS, 21, rue E. Solvay (C3), 4000 Liege, Belgium

<http://isis.ltas.ulg.ac.be/golinval/page.html>

Abstract

The paper develops a method for the parameter identification of massive piezoelectric structures. It can be shown that the piezoelectric effect involves a modification of the stiffness of the structure due to the coupling between the mechanical and electrical degrees of freedom. The behaviour of the structure is then dependent of the electrical conditions of the structure. A finite element model of the structure is the starting point of the studies to emphasise the stiffening by the piezoelectric effect. The initial mechanical FE model may be improved by adding elementary stiffness corrections to the global mechanical stiffness. These corrections depend on the piezoelectric properties of the material. External force excitation may be applied on the structure in two different electrical states in order to measure the forced responses. The identification problem becomes then a standard model updating problem which can be solved using well established techniques. However, particular attention has to be paid to the correction process to improve the knowledge of the structural behaviour without losing physical insight. Numerical examples illustrate the feasibility of the proposed method.

1. Introduction

Piezoelectricity is a fundamental process of electromechanical interaction [1]. There are two fundamental electromechanical effects associated with piezoelectricity, namely the direct effect and the converse effect. Direct effect can be detected when applying a force on a piezoelectric material and monitoring the electrical voltage or charge generated. Inversely, to emphasise the converse effect, an electric field can be applied to the material which will induce stress or strain. Piezoelectricity is used for a large number of applications in the field of electromechanical engineering, e.g. waves-sound generators, echographic probes, micro-positioner, accelerometer transducers, pressure transducers,... The success of active opto-mechanical devices has also emphasised the generalisation of the use of piezoelectric materials.

This fact has drawn much attention on how to accurately identify and monitor the piezoelectric coupling parameters, especially on structures having a partition of piezoelectric material which is not marginal versus the purely mechanical part. These

structures can be defined as *massively piezoelectric structures*.

In this paper, it will be shown that the piezoelectric effect involves a modification of the stiffness due to the coupling between the mechanical and electrical degrees of freedom (d.o.f.'s). Taking this behaviour into account, a method for the identification of the piezoelectric coupling parameters will be proposed : an initial mechanical finite element model (F.E.) will be improved by adding elementary stiffness corrections to the global mechanical stiffness. These corrections will depend on the piezoelectric parameters of the material. By applying an external force excitation on the structure, the forced response, depending of the electrical state of the structure, will be measured. Performing a model updating procedure results in a model behaving like the measures with an improved knowledge of the structure behaviour without losing physical insight. A numerical example of a piezoelectric bar will illustrate the feasibility of a piezoelectric model correction. Emphasis will be done on the numerical problems inherent to the bad numerical conditioning between mechanical and piezoelectric partitions and solutions will be proposed to overcome these difficulties.

2. Modelisation of Piezoelectricity

2.1 Piezoelectric Constitutive Equations

Linear piezoelectricity is described by the following equations [2]:

$$\begin{cases} \mathbf{T} = \mathbf{C}^E \mathbf{S} - \mathbf{e}^t \mathbf{E} \\ \mathbf{D} = \mathbf{e} \mathbf{S} + \boldsymbol{\varepsilon}^s \mathbf{E} \end{cases} \quad (1)$$

where

- \mathbf{T} = 6x1 stress vector,
- \mathbf{S} = 6x1 strain vector,
- \mathbf{D} = 3x1 electrical displacement vector,
- \mathbf{E} = 3x1 electrical field vector,
- \mathbf{C}^E = 6x6 elasticity matrix
(at constant electric field),
- \mathbf{e} = 3 x 6 piezoelectric matrix,
- $\boldsymbol{\varepsilon}^s$ = 3 x 3 dielectric matrix
(at constant deformation).

The electrical and mechanical balances will complete this set of fundamental equations of piezoelectricity :

- the electrical field \mathbf{E} is linked to the electrical potential φ by

$$\mathbf{E} = -\nabla\varphi \quad (2)$$

- for an electrical insulator, the Gauss theorem express the conservation of electrical charges as

$$\nabla \mathbf{D} = 0 \quad (3)$$

- the Newton's law express the force balance as

$$\rho \frac{\partial^2 \mathbf{U}}{\partial t^2} = \nabla \mathbf{T} \quad (4)$$

with

ρ the mass density,

∇ the divergence operator,

\mathbf{U} the 3x1 displacement vector, linked to the deformation vector by

$$\mathbf{S}_{ij} = \frac{1}{2} \left(\frac{\partial \mathbf{U}_i}{\partial \mathbf{x}_j} + \frac{\partial \mathbf{U}_j}{\partial \mathbf{x}_i} \right) = (\hat{\nabla} \mathbf{U})_{ij} \quad (5)$$

Equations (1) to (5) constitute a piezoelectric model which is practically impossible to solve directly due to the complexity of this set of differential equations.

2.2 Finite Element Formulation

The first step is to operate a discretisation of the piezoelectric medium into volume elements and to express :

- the mechanical displacements \mathbf{U} in terms of nodal values by

$$\mathbf{U} = \mathbf{N}_u \mathbf{U}_i \quad (6)$$

with

\mathbf{U}_i displacement at node i

\mathbf{N}'' interpolation matrix of displacements;

- the electrical potentials φ in terms of nodal values by:

$$\varphi = \mathbf{N}_\phi \varphi_i \quad (7)$$

with

φ_i potential at node i ,

\mathbf{N}_ϕ interpolation vector of potentials,

The second step is to transform the differential problem (1) - (5) into an integral form on the discretised volumes. Defining the differential operator \mathbf{B} as :

$$\mathbf{B} = \begin{pmatrix} \frac{\partial}{\partial \mathbf{x}} & \mathbf{0} & \mathbf{0} & \frac{\partial}{\partial \mathbf{y}} & \mathbf{0} & \frac{\partial}{\partial \mathbf{z}} \\ \mathbf{0} & \frac{\partial}{\partial \mathbf{y}} & \mathbf{0} & \frac{\partial}{\partial \mathbf{x}} & \frac{\partial}{\partial \mathbf{z}} & \mathbf{0} \\ \mathbf{0} & \mathbf{0} & \frac{\partial}{\partial \mathbf{z}} & \mathbf{0} & \frac{\partial}{\partial \mathbf{y}} & \frac{\partial}{\partial \mathbf{x}} \end{pmatrix}^t \quad (8)$$

the following elementary contributions are obtained

- the mechanical inertia :

$$\mathbf{M}_{UU}^{vol} = \iiint \rho \mathbf{N}_u^t \mathbf{N}_u \, dV \quad (9)$$

- the elastic coupling :

$$\mathbf{K}_{UU}^{vol} = \iiint (\mathbf{B} \mathbf{N}_u)^t \mathbf{C}^E \mathbf{B} \mathbf{N}_u \, dV \quad (10)$$

- the piezoelectric coupling :

$$\mathbf{K}_{U\phi}^{vol} = \iiint (\mathbf{B} \mathbf{N}_u)^t \mathbf{e}^t \nabla \mathbf{N}_\phi \, dV \quad (11)$$

- the dielectric coupling :

$$\mathbf{K}_{\phi\phi}^{vol} = -\iiint (\nabla \mathbf{N}_\phi)^t \boldsymbol{\varepsilon}^s \nabla \mathbf{N}_\phi \, dV \quad (12)$$

- the electrical charges at electrodes :

$$\mathbf{Q}^{vol} = -\iint \mathbf{N}_\phi^t \boldsymbol{\sigma} \, dS \quad (13)$$

- the mechanical forces applied on the volume :

$$\mathbf{F}^{\text{vol}} = \iiint \mathbf{N}_u^t \mathbf{P}_v dV + \iint \mathbf{N}_u^t \mathbf{P}_s dS + \mathbf{N}_u^t \mathbf{P}_n \quad (14)$$

where \mathbf{P}_v , \mathbf{P}_s , \mathbf{P}_n represent respectively the volume, surface and nodal forces and σ is the electrical charge density on electrodes.

The assembling of the elementary matrices (9) to (14) leads to a system of equations which is the 3-D F.E. representation of an undamped piezoelectric structure :

$$\begin{pmatrix} \mathbf{M}_{UU} & \mathbf{0} & \mathbf{0} \\ \mathbf{0} & \mathbf{0} & \mathbf{0} \\ \mathbf{0} & \mathbf{0} & \mathbf{0} \end{pmatrix} \begin{pmatrix} \ddot{\mathbf{U}} \\ \ddot{\phi}_i \\ \ddot{\phi}_{el} \end{pmatrix} + \begin{pmatrix} \mathbf{K}_{UU} & \mathbf{K}_{U\phi_i} & \mathbf{K}_{U\phi_{el}} \\ \mathbf{K}_{U\phi_i}^t & \mathbf{K}_{\phi_i\phi_i} & \mathbf{K}_{\phi_i\phi_{el}} \\ \mathbf{K}_{U\phi_{el}}^t & \mathbf{K}_{\phi_i\phi_{el}}^t & \mathbf{K}_{\phi_{el}\phi_{el}} \end{pmatrix} \begin{pmatrix} \mathbf{U} \\ \phi_i \\ \phi_{el} \end{pmatrix} = \begin{pmatrix} \mathbf{F} \\ \mathbf{0} \\ \mathbf{Q}_{el} \end{pmatrix} \quad (15)$$

where subscript **i** is referred for 'internal' electrical d.o.f.'s and subscript **el** for electrical d.o.f.'s at the electrodes of the structure (figure 1).

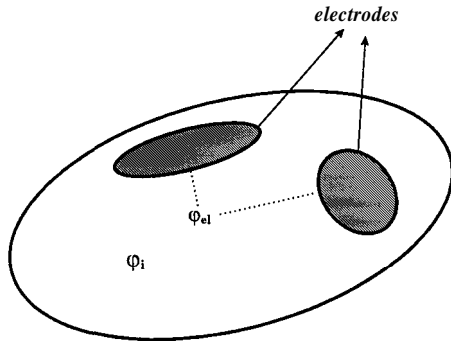


Figure 1: Electrodes on structure

Four important remarks have to be done regarding to equation (15) :

- no terms of inertia are associated with the electrical d.o.f.'s;
- the piezoelectric stiffness matrix is symmetric;
- some experiments have shown a small complex part of the piezoelectric coefficients, involving an imaginary partition of the stiffness matrix; the theory developed here is based on the assumption of a non damped model;
- due to the Gauss theorem applied on an insulated material, electrical charges only exist at the electrode level.

In order to simplify equation (15), a condensation of the internal electrical potential, ϕ_i may be performed using a **Guyan** static reduction [4]:

$$\begin{pmatrix} \mathbf{M}_{UU} & \mathbf{0} \\ \mathbf{0} & \mathbf{0} \end{pmatrix} \begin{pmatrix} \ddot{\mathbf{U}} \\ \ddot{\phi}_{el} \end{pmatrix} + \begin{pmatrix} \mathbf{H}_{UU} & \mathbf{H}_{U\phi_{el}} \\ \mathbf{H}_{U\phi_{el}}^t & \mathbf{H}_{\phi_{el}\phi_{el}} \end{pmatrix} \begin{pmatrix} \mathbf{U} \\ \phi_{el} \end{pmatrix} = \begin{pmatrix} \mathbf{F} \\ \mathbf{Q}_{el} \end{pmatrix} \quad (16)$$

where $\mathbf{H}_{UU} = \mathbf{K}_{UU} - \mathbf{K}_{U\phi_i} \mathbf{K}_{\phi_i\phi_i}^{-1} \mathbf{K}_{U\phi_i}^t$

$$\mathbf{H}_{U\phi_{el}} = \mathbf{K}_{U\phi_{el}} - \mathbf{K}_{U\phi_i} \mathbf{K}_{\phi_i\phi_i}^{-1} \mathbf{K}_{\phi_i\phi_{el}}^t$$

$$\mathbf{H}_{\phi_{el}\phi_{el}} = \mathbf{K}_{\phi_{el}\phi_{el}} - \mathbf{K}_{\phi_i\phi_{el}}^t \mathbf{K}_{\phi_i\phi_i}^{-1} \mathbf{K}_{\phi_i\phi_{el}}$$

Note that the condensation of the internal d.o.f.'s is exact since no terms of inertia are associated with the ϕ_i .

2.3 Electrical Boundary Conditions

Two kinds of electrical boundary conditions [2] can be prescribed, which involve two different stiffness matrices [3]:

1) *Conditions on electrical charges \mathbf{Q}_{el} .*

In this case, potentials ϕ_{el} are directly linked to displacements \mathbf{U} by the second equation of (16), involving :

$$\mathbf{M}_{UU} \ddot{\mathbf{U}} + (\mathbf{H}_{UU} - \Delta\mathbf{H}) \mathbf{U} = -\mathbf{H}_{U\phi_{el}} \mathbf{H}_{\phi_{el}\phi_{el}}^{-1} \mathbf{Q}_{el} + \mathbf{F} \quad (17)$$

where $\Delta\mathbf{H} = \mathbf{H}_{U\phi_{el}} \mathbf{H}_{\phi_{el}\phi_{el}}^{-1} \mathbf{H}_{U\phi_{el}}^t$

Physically, this condition results from a short-circuit of the electrodes. It can be performed by connecting them to a charge amplifier or by exciting the piezoelectric structure in current.

2) *Conditions on the potentials ϕ_{el} .*

In the first equation of (16), the electrical potentials can be considered as excitation, involving :

$$\mathbf{M}_{UU} \ddot{\mathbf{U}} + \mathbf{H}_{UU} \mathbf{U} = -\mathbf{H}_{U\phi_{el}} \phi_{el} + \mathbf{F} \quad (18)$$

Physically, this condition corresponds to an open circuit of the electrodes. It can be performed by connecting them to a voltmeter or by exciting the piezoelectric structure in voltage.

From equations (17) and (18), it is interesting to notice that the coupling between the mechanical and electrical d.o.f.'s induces a stiffening effect of the structure. Naillon et al. [2], have shown that the eigen frequencies of a piezoelectric structure with boundary conditions on the electrode potentials are always smaller than the corresponding eigen

frequencies with boundary conditions on the electrode electrical charges. Moreover, these two sets of 'piezoelectric' eigen frequencies are always greater than for a purely mechanical structure with the same geometry and same mechanical boundary conditions.

2.4 Example: the Piezoelectric Bar

In order to illustrate the piezoelectric effects, a numerical simulation has been performed on the example of a piezoelectric bar, clamped at one side, and excited by a mechanical force at the other side as presented in figure 2.

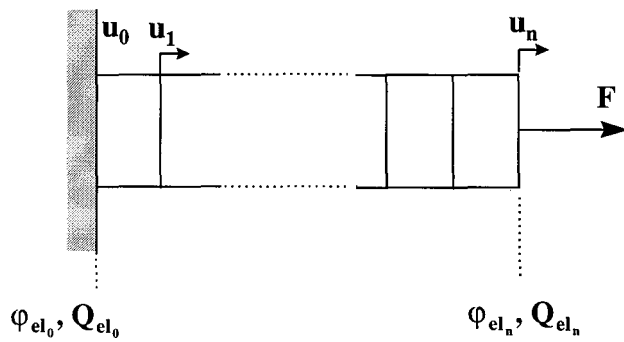


Figure 2: Piezoelectric bar in extension

Table 1 shows the physical parameters used in this numerical test-case.

	Values	Unit
Bar radius	0.0025	m
Bar length	0.2	m
Young modulus	$62.5 \cdot 10^7$	N/m ²
Mass density	7500	kg/m ³
Piezo cst. $e(3,3)$	14.1	C/m ²
Dielectric cst. $\epsilon^s(3,3)$	$5.84 \cdot 10^{-9}$	F/m

Table 1: Piezoelectric bar parameters

In figure 3, the frequency response function at the end side of the bar is presented for three different cases (purely mechanical structure, piezo-structure with electrodes in open circuit, piezo-structure with electrodes in short circuit).

Figure 3 and table 2 emphasise the frequency shifts and the influence of the piezoelectric coupling on the static stiffness.

The correlation between the eigen modes of a purely mechanical structure and the eigen modes of the same structure but considered as piezoelectric may be calculated using the MAC matrix defined by equation (19).

mode n°	open-circuit	short-circuit
1	2.1%	13.9%
2	12.6%	13.9%
3	13.3%	13.9%

Table 2: Relative frequency shifts for the piezoelectric material with respect to the purely mechanical structure

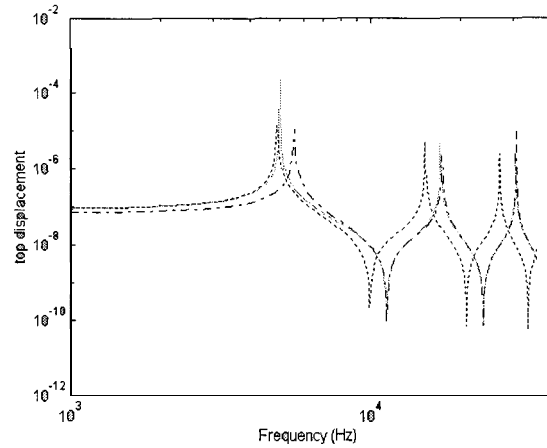


Figure 3: Stiffening effect on a piezoelectric clamped bar

- Mechanical structure
- - - Electrodes in open circuit
- · - Electrodes in short-circuit

$$MAC = \frac{\left| \left\{ \phi_{piezo} \right\}_i^t \left\{ \phi_{mech}^* \right\}_j \right|^2}{\left(\left\{ \phi_{piezo} \right\}_i^t \left\{ \phi_{piezo}^* \right\}_i \right) \left(\left\{ \phi_{mech} \right\}_j^t \left\{ \phi_{mech}^* \right\}_j \right)} \quad (19)$$

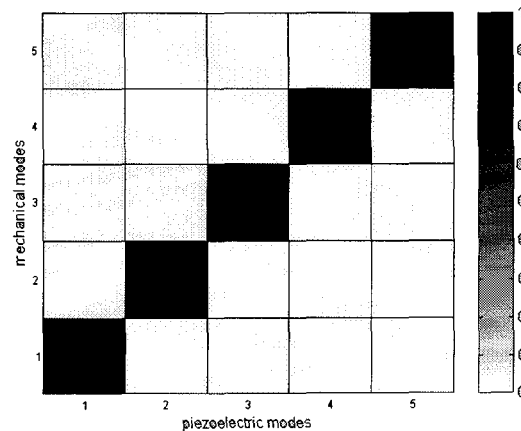


Figure 4: MAC matrix between purely mechanical modes and piezoelectric modes

As shown in figure 4, a perfect correlation exists between the eigen modes of the purely mechanical structure and the piezoelectric structure. This means that, in the example of the piezoelectric bar, the piezoelectric effect does not change the modal shapes, but only induces a frequency shift. It is important to notice that, in the case of a structure with partitions of piezoelectric material and partitions of purely mechanical material, this conclusion remains no longer valid since the piezoelectric parts will induce local changes of stiffness which will certainly perturb the initial purely mechanical mode shapes.

3. Scaling of the Piezoelectric Stiffness Matrix

3.1 Order of Magnitude of the Stiffness Matrix Coefficients

In equation (15), the stiffness matrix

$$\mathbf{K}_{\text{coupled}} = \begin{pmatrix} \mathbf{K}_{\text{UU}} & \mathbf{K}_{\text{U}\phi_i} & \mathbf{K}_{\text{U}\phi_{el}} \\ \mathbf{K}_{\text{U}\phi_i}^t & \mathbf{K}_{\phi_i\phi_i} & \mathbf{K}_{\phi_i\phi_{el}} \\ \mathbf{K}_{\text{U}\phi_{el}}^t & \mathbf{K}_{\phi_i\phi_{el}}^t & \mathbf{K}_{\phi_{el}\phi_{el}} \end{pmatrix} \quad (20)$$

exhibits terms with different orders of magnitude. The elastic terms have generally a magnitude of 10^{10} , in comparison with 10^0 for the piezo-elastic coupling terms and with 10^{-10} for the dielectric terms.

$$\mathbf{K}_{\text{coupled}} \doteq \begin{pmatrix} \begin{bmatrix} \ddots & \vdots & \ddots \\ \dots & 10^{10} & \dots \\ \ddots & \vdots & \ddots \\ \dots & 10^0 & \dots \\ \ddots & \vdots & \ddots \end{bmatrix} & \begin{bmatrix} \ddots & \vdots & \ddots \\ \dots & 10^0 & \dots \\ \ddots & \vdots & \ddots \\ \dots & 10^{-10} & \dots \\ \ddots & \vdots & \ddots \end{bmatrix} \end{pmatrix}$$

This numerical ill-conditioning of the piezoelectric stiffness matrix requires some cares [5] for the resolution of equations (15), (17) or (18).

3.2 Scaling Method

To overcome this problem, one solution is to scale the stiffness matrix $\mathbf{K}_{\text{coupled}}$ by constructing a diagonal matrix \mathbf{P} which contains the square root of

the diagonal terms of $\mathbf{K}_{\text{coupled}}$. For example, the static problem:

$$\mathbf{K}_{\text{coupled}} \mathbf{x} = \mathbf{F} \quad (21)$$

can be transformed by using the following relations:

$$\begin{aligned} \mathbf{P} \mathbf{P}^{-1} \mathbf{K}_{\text{coupled}} \mathbf{P}^{-1} \mathbf{P} \mathbf{x} &= \mathbf{F} \\ \downarrow \\ \mathbf{P}^{-1} \mathbf{K}_{\text{coupled}} \mathbf{P}^{-1} \mathbf{P} \mathbf{x} &= \mathbf{P}^{-1} \mathbf{F} \\ \downarrow \\ \mathbf{K}_{\text{scaled}} \mathbf{x}_{\text{scaled}} &= \mathbf{F}_{\text{scaled}} \end{aligned} \quad (22)$$

where

$$\mathbf{K}_{\text{scaled}} = \mathbf{P}^{-1} \mathbf{K}_{\text{coupled}} \mathbf{P}^{-1} \quad (23)$$

$$\mathbf{x}_{\text{scaled}} = \mathbf{P} \mathbf{x} \quad (24)$$

$$\mathbf{F}_{\text{scaled}} = \mathbf{P}^{-1} \mathbf{F} \quad (25)$$

After transformation, equation (22) exhibits a good numerical conditioning.

The eigen value problem resulting from the piezoelectric system (15) can also be conditioned using the same procedure. It gives :

$$\left(\mathbf{K}_{\text{scaled}} - \omega^2 \mathbf{M}_{\text{scaled}} \right) \mathbf{P} \begin{pmatrix} \mathbf{U} \\ \phi_i \\ \phi_{el} \end{pmatrix} = \mathbf{0} \quad (26)$$

with

$$\mathbf{M}_{\text{scaled}} = \mathbf{P}^{-1} \mathbf{M}_{\text{piezo}} \mathbf{P}^{-1} \quad (27)$$

3.3 Singular Value Decomposition

As discussed in §3.1, the magnitude difference of the piezoelectric stiffness matrix coefficients could induce ill-conditioning and numerical instabilities when solving static and dynamic problems or-when performing model updating on piezoelectric structure. A solution is to filter out instabilities using the well-known singular value decomposition (SVD) algorithm and to reject singular values that are smaller than an average threshold [6]. For example, in the case of the resolution of the static problem (21) :

$$\mathbf{K}_{\text{coupled}} \mathbf{x} = \mathbf{F}$$

the stiffness matrix is factored as :

$$\mathbf{K}_{\text{coupled}} = \mathbf{U}\mathbf{\Sigma}\mathbf{V}^t \quad (28)$$

where

- U and V are orthogonal matrices which contain the left and right singular vectors,
- $\mathbf{\Sigma}$ is a diagonal matrix that contains the singular values σ_i of $\mathbf{K}_{\text{coupled}}$ which are representative of the ill-conditioning.

The advantage of the SVD algorithm is that if a line or a row i of $\mathbf{K}_{\text{coupled}}$ is not totally linearly dependent, we would obtain a small value for σ_i , instead of zero. Therefore, it is easy to establish a criterion for the rejection of small singular values by comparing them for example to a threshold proportional to the singular value average :

$$\sigma_{\text{threshold}} = 10^{-q} \frac{1}{N} \sum_{i=1 \dots N} \sigma_i \quad (29)$$

where q is a user defined integer and N is the number of non-zero singular values of $\mathbf{K}_{\text{piezo}}$. Using the filtered singular values of $\mathbf{\Sigma}$ and the orthogonality properties of U and V, the inversion of problem (21) becomes easy. Note that this procedure is also widely used in the case of the resolution of over-determined systems.

4. Identification of the Piezo-electric Coupling Parameters

In order to identify the piezoelectric coupling coefficients of a structure, it is possible to start with the finite element model of the non piezoelectric structure and to correct it using experimental data. This updating procedure allows to build a model that improves the knowledge of the structure without losing physical insight. In the following, two well established updating techniques will successfully applied the example of a piezoelectric structures taking into account scaling problems mentioned previously.

4.1 FRF-based Updating Procedure

The finite element model updating method described hereafter [7-8] is based on the existence of two discretized experimental stiffness $[\mathbf{K}_x]$ and mass $[\mathbf{M}_x]$ matrices that have the same properties as the corresponding analytical matrices $[\mathbf{K}_a]$ and

$[\mathbf{M}_a]$ (in terms of symmetry, connectivity,...) and such that the dynamic equilibrium equation is satisfied, using measured frequency responses, i.e. :

$$[\mathbf{K}_x] \{\mathbf{H}_x\}_j = \omega_x^2 [\mathbf{M}_x] \{\mathbf{H}_x\}_j + \{\mathbf{f}\} \quad (30)$$

where

- $\{\mathbf{H}_x\}_j$ is the j -th experimental FRF vector measured at frequency ω_x ,
- $\{\mathbf{f}\}$ is the vector of excitation forces.

In the following, the notations $[\dots]$ and $\{\dots\}$ will be used to emphasise respectively matrices and vectors; subscripts a and x will relate to the analytical and experimental quantities respectively.

It is also assumed that the matrix corrections take the form :

$$[\Delta\mathbf{Z}(\omega, \{\Delta\mathbf{p}\})] = \frac{\partial [\mathbf{Z}_a(\omega)]}{\partial \{\mathbf{p}\}} \otimes \{\Delta\mathbf{p}\} \quad (31)$$

where

- $[\mathbf{Z}_a(\omega)]$ states for the dynamic stiffness matrix,
- $\{\Delta\mathbf{p}\}$ is defined as the vector of updating parameters,
- \otimes refers to the Kronecker product.

In the following, the inadequacy of the finite element model will be expressed in terms of N_p error elementary stiffness matrices in the form [4] :

$$[\Delta\mathbf{K}] = \sum_{i=1}^{N_p} \Delta\mathbf{p}_i [\mathbf{K}_{\text{elem}}]_i \quad (32)$$

This assumption leads directly to the expression of the stiffness sensitivity in the form :

$$\frac{\partial [\mathbf{Z}_a(\omega)]}{\partial \mathbf{p}_i} = [\mathbf{K}_{\text{elem}}]_i \quad (33)$$

The dynamic stiffness matrix correction can also be expressed as :

$$[\Delta\mathbf{Z}(\omega, \{\Delta\mathbf{p}\})] = [\mathbf{Z}_x(\omega)] - [\mathbf{Z}_a(\omega)] \quad (34)$$

Pre-multiplying this equation by the analytical FRF matrix $[\mathbf{H}_a(\omega)]$ and post-multiplying by an experimental FRF vector $\{\mathbf{H}_x(\omega)\}_j$ yields to the following over-determined system of equations (the number of equations depending of the number of

measured points at N_ω different frequencies) in terms of the unknown vector $\{\mathbf{Ap}\}$:

$$[\mathbf{H}_a(\omega)][\Delta\mathbf{Z}(\omega, \{\Delta\mathbf{p}\})]\{\mathbf{H}_x(\omega)\}_j = \{\mathbf{H}_a(\omega)\}_j - \{\mathbf{H}_x(\omega)\}_j \quad (35)$$

which can be easily solved by least square techniques.

4.2 Updating Method Based on Modal Parameters

In this approach, model updating is performed using the experimental mode shapes [9]. As only a subset of the model co-ordinates are actually measured, this procedure requires an expansion of the experimental eigen vectors to the size of the finite element model eigen vectors.

The expansion method may be achieved using a method based on the minimisation of errors on the constitutive equations, which results in the following objective function :

$$\min(\{\mathbf{U}\} - \{\mathbf{V}\})^T [\mathbf{K}] (\{\mathbf{U}\} - \{\mathbf{V}\}) + \alpha (\{\mathbf{V}_1\} - \{\bar{\mathbf{V}}\})^T [\mathbf{K}_{red}] (\{\mathbf{V}_1\} - \{\bar{\mathbf{V}}\}) \quad (36)$$

where

- $\{\bar{\mathbf{V}}\}$ is the experimental eigen vector,
- $\{\mathbf{V}\}$ is the experimental expanded eigen vector,
- $\{\mathbf{V}_1\}$ is the measured partition of $\{\mathbf{V}\}$,
- $\{\mathbf{U}\}$ is an instrument eigen vector that verifies *a priori* the equilibrium equations :

$$[\mathbf{K}_a]\{\mathbf{U}\} = \omega^2 [\mathbf{M}_a]\{\mathbf{V}\} \quad (37)$$

- $[\mathbf{K}_{red}]$ is the analytical stiffness matrix reduced to the partition of measured degrees of freedom,
- α is a user defined weighting coefficient that indicates confidence in the measurements.

If the existence of experimental mass and stiffness matrices that satisfy equilibrium equation is assumed :

$$[\mathbf{K}_x]\{\mathbf{V}\} = \omega^2 [\mathbf{M}_x]\{\mathbf{V}\} \quad (38)$$

the following system can be found for parameter corrections :

$$[\mathbf{K}]^{-1}[\Delta\mathbf{Z}(\omega, \Delta\mathbf{p})]\{\mathbf{V}\} = \{\mathbf{U}\} - \{\mathbf{V}\} \quad (39)$$

where

$$[\Delta\mathbf{Z}(\omega, \Delta\mathbf{p})] = [\Delta\mathbf{K}(\Delta\mathbf{p})] - \omega^2 [\Delta\mathbf{M}(\Delta\mathbf{p})] \quad (40)$$

is the correction matrix for the dynamic stiffness.

Updating may be performed using the same development as in equation (32).

More details about the updating methods presented in sections 4.1 and 4.2 can be found in references [8] and [9].

4.3 Numerical example

The piezoelectric bar model, described in section 2.4 is used to demonstrate the ability of the FRF and modal response based updating methods to identify the piezoelectric coupling parameters in the stiffness matrix.

The clamped bar is discretised with 5 elements leading to 5 mechanical degrees of freedom and 5 electrical degrees of freedom (the clamped side of the electrode is assumed to be grounded). Experimental data are generated using the complete piezoelectric 'true' model. In order to take into account the incompleteness of experimental data, only the frequency range covered by the 3 first modes is considered and only **half** of the displacement d.o.f.'s along with the electrode (voltage or charges) are assumed to be monitored.

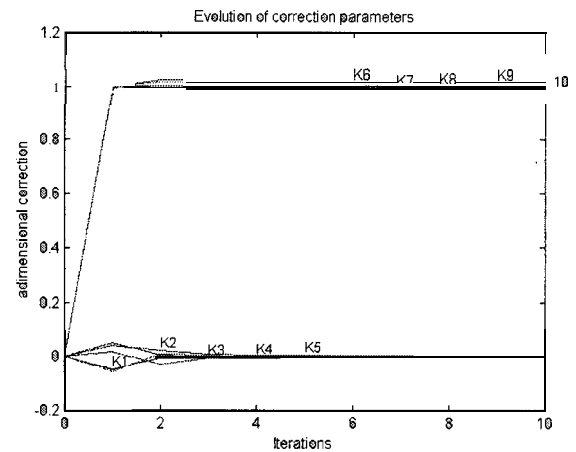


Figure 5: Analytical model correction using FRF (no noise data, no structural damping)

The 'analytical' model was generated by withdrawing completely the piezoelectric partition of the bar model given in equation (15).

Updating results are presented in figures 5 and 6. The modal response based updating technique gives

a perfect result while the FRF based method exhibits less than 0.35% error.

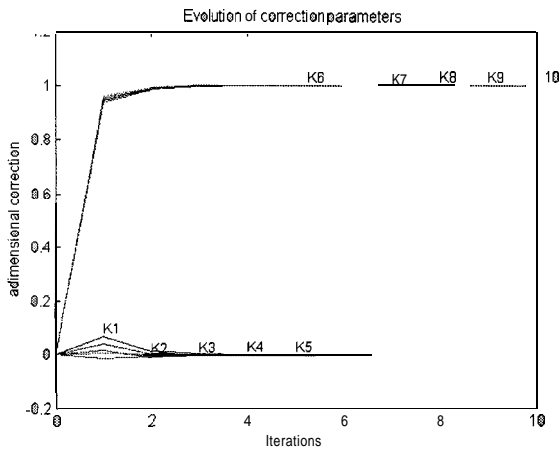


Figure 6: Analytical model correction using modes (no noise data, no structural damping)

The mechanical stiffness correction (K1 to K5) is 0 since the ‘analytical’ model has 0% of error on mechanical stiffness. The piezoelectric stiffness correction (K6 to K10) is 1 since the ‘analytical’ model has 100% of error on piezoelectric stiffness.

Figure 7 presents the ‘realistic’ FRF’s generated by introducing 1% of modal damping and 1/1000 noise factor on the maximum acceleration.

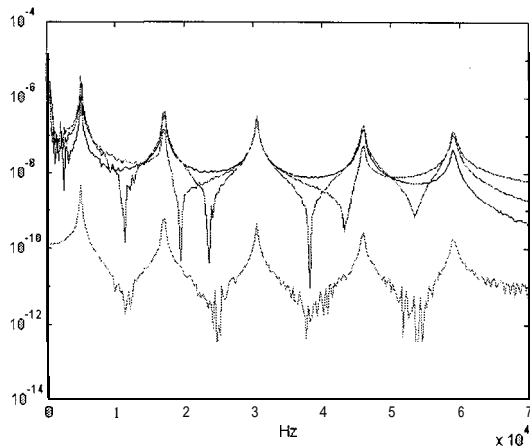


Figure 7: Noisy FRF's on the damped system

In this case, the FRF based method exhibits an error of 10% while the modal response based procedure achieves less than 7.2%. As shown in figure 8, the introduction of damping and the presence of noise induces mechanical stiffness residues that perturb the identification of piezoelectric coefficients.

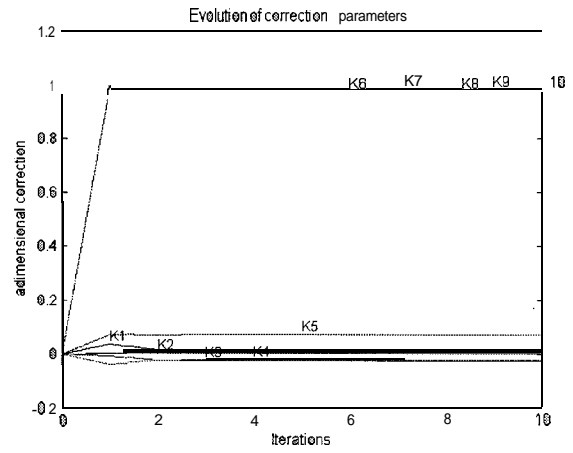


Figure 8: Analytical model correction using modes (noisy data, structural damping)

A modal parameter based updating has also been performed starting from an initial perturbed model in which the mechanical stiffness of element 3 (K3) was raised by 50%. Figure 9 shows the success of the model correction where a maximum of 13% of error has been achieved using ‘realistic’ data.

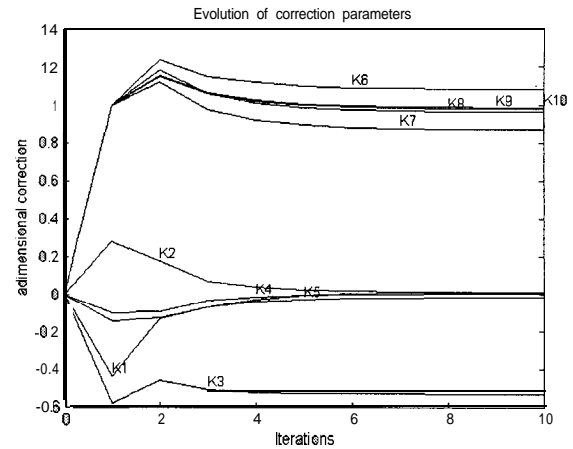


Figure 9: Piezoelectric and stiffness model correction using modes (noisy data, structural damping)

5. Conclusion

An identification method of the coupling parameters of a massively piezoelectric structure based on model updating techniques was presented.

Numerical ill-conditioning problems resulting from piezoelectric modelling were taken into account in the different steps of the model correction procedures in order to improve convergence :

- scaling of the piezoelectric stiffness matrix before reduction (or expansion) of the experimental mode shapes,
- solution of the pre-scaled eigenvalue problem,
- solution of the least squared problem using the SVD filtering technique.

Influence of noise and damping on experimental data has also been shown for the piezoelectric and stiffness model correction procedures.

References

1. T. Ikeda, **Fundamentals of piezoelectricity**, Oxford Science Publications (1996).
2. M. Naillon, R.H. Coursant, F. Besnier, **Analyse de structures piézoélectriques par une méthode d'éléments finis**, ACTA Electronica, Vol. 25, No. 4, pp. 341-362 (1983).
3. D. Boucher, M. Lagier, C. Maerfield, **Computation of the vibrational modes for piezoelectric array transducers using a mixed finite element-perturbation method**, IEEE Transactions on sonics and ultrasonics, Vol. SU-28, No. 5 (1981).
4. N.M.M. Maia, J.M.M. Silva et al, **Theoretical and experimental modal analysis**, Research studies press ltd., John Wiley & Sons Inc. (1997).
5. Y.-K. Yong, Y. Cho, **Numerical algorithms for solutions of large eigenvalues problems in piezoelectric resonators**, International journal for numerical methods in engineering., Vol. 39, pp. 909-922 (1996).
6. F.M. Hemez, C. Farhat, **Bypassing numerical difficulties associated with updating simultaneous mass and stiffness matrices**, AIAA Journal, Vol. 33, No. 3, pp. 539-546 (1995).
7. P. Larsson, **Model updating based on forced vibrations**, Proceedings of the Chuo-K.U. Leuven U.C. Seminar, Tokyo, Japan (1991).
8. R. Pascual, J.-C. Golinval, **A model updating method based on the concept of frequency shift between analytical and experimental FRFs**, 6th Biennial Conference on Mechanical Vibration and Noise, September 14-17, 1997, Sacramento, California
9. P. Collignon, R. Pascual, J.-C. Golinval, **Model updating strategies adapted to structural failure detection**, Proceedings of the 4th congress of theoretical and applied mechanics, Leuven (1997).